

Thermo/hydration responsive shape memory polymers with enhanced hydrophilicity for biomedical applications

Yuta Suzuki^{1,2}, Qichan Hu³, Benjamin Batchelor⁴, Walter Voit¹  and Melanie Ecker^{3,*} 

¹ Department of Materials Science and Engineering, The University of Texas at Dallas, 800 W. Campbell Road Richardson, TX 75080, United States of America

² Research Center, Lintec Corporation, 5-14-42 Nishiki-cho, Warabi-shi, Saitama 335-0005, Japan

³ Department of Biomedical Engineering, University of North Texas, 3940 N Elm St, Denton, TX 76207, United States of America

⁴ Adaptive 3D Technologies, 608 Development Dr, Plano, TX 75074, United States of America

E-mail: melanie.ecker@unt.edu

Received 24 August 2022, revised 18 November 2022

Accepted for publication 23 November 2022

Published 5 December 2022



CrossMark

Abstract

Thiol-ene/acrylate shape memory polymers (SMPs) have sufficient stiffness for facile insertion and precision placement and soften after exposure to physiological conditions to reduce the mechanical mismatch with body tissue. As a result, they have demonstrated excellent potential as substrates for various flexible bioelectronic devices, such as cochlear implants, nerve cuffs, cortical probes, plexus blankets, and spinal cord stimulators. To enhance the shape recovery properties and softening effect of SMPs under physiological conditions, we designed and implemented a new class of SMPs as bioelectronics substrates. In detail, we introduced dopamine acrylamide (DAc) as a hydrophilic monomer into a current thiol-ene polymer network. Dry and soaked dynamic mechanical analyses were performed to evaluate the thermomechanical properties, softening kinetics under wet conditions, and shape recovery properties. Modification of SMPs by DAc provided an improved softening effect and shape recovery speed under physiological conditions. Here, we report a new strategy for designing SMPs with enhanced shape recovery properties and lower moduli than previously reported SMPs under physiological conditions without sacrificing stiffness at room temperature by introducing a hydrophilic monomer.

Supplementary material for this article is available [online](#)

Keywords: shape memory polymer, softening polymers, implantable devices, biomedical devices, neural interfaces, biomaterials, bioelectronics

(Some figures may appear in colour only in the online journal)

* Author to whom any correspondence should be addressed.



Original content from this work may be used under the terms of the [Creative Commons Attribution 4.0 licence](#). Any further distribution of this work must maintain attribution to the author(s) and the title of the work, journal citation and DOI.

1. Introduction

Neural interfaces are being actively studied and commercialized owing to their ability to diagnose and treat various diseases and disorders by stimulating nerves and recording nervous activity for replacement, recovery, or observation of neurological functions [1]. Numerous bioelectronic devices have been widely used and are under investigation to improve the lives of people suffering from disabilities and diseases [2]. Some devices, such as electrocorticography arrays [3], electrocardiogram devices [4], and nerve cuffs [5], are implanted in the body to obtain a higher spatial resolution and signal-to-noise ratio. Traditional implantable devices are fabricated on silicon or metal substrates, which have excellent electrical properties and durability and are suitable for semiconductor fabrication processes [6, 7]. However, the moduli of silicon and metals (>100 GPa) are orders of magnitude larger than the body tissues with which they interface (storage moduli (E') are 1 MPa, 100–10 kPa, and 100–1500 kPa for dura mater, spinal cord, and neural tissues, respectively). The large mechanical mismatch between stiff devices and soft body tissue induces foreign body responses (e.g. encapsulation of the device by scar tissue and chronic inflammation), which degrade the device's performance for long-term implantation [8]. To reduce the mismatch [9], polymer-based devices employing polyimides [10] ($E' = 2.5$ GPa), parylene C [11] ($E' = 3$ GPa), and SU-8 [12] ($E' = 3$ GPa) have been developed, but a large mechanical mismatch still remains. Although polydimethylsiloxane substrates exhibit a sufficiently low E' (as low as 1–10 MPa) to significantly alleviate the mismatch problems [13], they are very difficult to handle and implant in the limited space for surgical implantation due to their lack of rigidity.

To address the problem, Voit's group has investigated thiol-ene/acrylate shape memory polymer (SMP) substrates whose mechanical properties are tunable by varying the monomer composition [14]. The SMPs are in their glassy state at room temperature, and their stiffness makes implantation easier. However, after implantation in the body and exposure to physiological conditions, they soften owing to the temperature increase and water uptake to decrease the mechanical mismatch. In addition to the softening property, the SMPs can change shape from a temporary to a permanent shape when exposed to physiological conditions. The recovery property provides a less invasive surgical approach especially when the devices have limited space for surgical implantation, such as for nerve cuffs and spinal cord stimulators [15, 16]. For example, the shape recovery effect enables initially flat nerve cuff devices that self-wrap around the target nerve to establish a conformal and robust electrical connection without undesired deformation and damage of the nerve [17]. The validity and usefulness of the SMPs as biomedical substrates has been demonstrated in previous research, including *in vivo* implantation tests [18]. However, there is a continuing need for better control of the softening mechanics of substrate materials to improve their utility to house neural interfaces.

Lowering the glass transition temperature (T_g) or cross-link density would provide a higher recovery ratio because the shape recovery effect of thermally responsive SMPs usually is more effective above T_g [19]. However, as mentioned above, it is desirable for SMP substrates to be stiff at room temperature; thus, controlling the mechanical properties by simply adding a soft segment or decreasing the crosslinking density is not a good strategy since it affects other important properties of the devices. In contrast, indirect heating through Joule heating using dispersed conductive materials, like carbon filler or carbon nanotubes [20, 21], or light exposure of photothermal materials have been reported to accelerate shape recovery [22]. Still, they complicate the implant procedure, and tissue damage is a concern.

In this work, we designed new SMPs to enhance the shape recovery ratio and softening effect under physiological conditions by incorporating a hydrophilic monomer into a current thiol-ene SMP system. Dopamine acrylamide (DAc), which has a catechol residue, was selected as the hydrophilic monomer to control the hydrophilicity and thermomechanical properties. The catechol group in DAc is not merely hydrophilic but also biocompatible [23]; it is used for adhesion-promoting coatings [24, 25] and scaffolds for several biomaterials [26]. We were inspired by Patton and his colleagues, who have pioneered work on adhesive thiol-ene polymers using DAc [27]. From their thermomechanical measurements, it was apparent that these thiol-ene polymers will exhibit shape memory properties due to the extensive change in storage modulus while going through their glass transition temperature (T_g). Their thiol-ene system used monomers with high rotational freedom, which resulted in polymers with relatively low glass transition temperatures (10 °C–36 °C). However, to achieve the softening described earlier for the application in neural interfaces, the solution space demands the creation of polymers with a higher initial T_g that will be able to change to a T_g like that described by Sparks *et al* [27] after water induced plasticization. This has historically presented a problem for thiol-based chemistries owing to the rotational flexibility of thio-ester linkages, which typically drive T_g to body temperature or below. Beyond this challenge which we solve through polymer network design, our focus is on the shape memory properties of these polymers rather than on the adhesive properties. We want to utilize water-induced plasticization to trigger the shape recovery of our polymers. DAc has received much attention in the published literature because it is an adhesive component of mussel foot proteins. Still, this biomimicry has unduly biased the community to focus primarily on the adhesive properties of these materials and shifted attention away from a host of other valuable properties that the sterics of this combination of chemical side chains provide to network polymers.

SMPs with various DAc monomer ratios were synthesized by copolymerization of DAc and thiol-ene monomers. Dry and soaked dynamic mechanical analysis (DMA) was performed to evaluate the mechanical properties of the modified SMPs under dry and wet conditions, respectively. The SMPs exhibited an improved shape recovery ratio and lower

T_g and E' under wet conditions with an increasing DAc ratio. A comparison with SMPs modified with phenethyl acrylamide (PAC), which has the same chemical structure as DAC except it lacks two adjacent hydroxyl groups, clearly showed enhanced hydrophilicity and reduced T_g and E' contributed to the improved recovery effect. Here, we optimize the hydrophilicity and thermomechanical properties of SMPs by incorporating a hydrophilic monomer to make SMP substrates more advantageous for biomedical applications.

2. Materials and methods

2.1. Materials

Triallyl-1,3,5-triazine-2,4,6-trione (TATATO), tris[2-(3-mercaptopropionyloxy)ethyl] isocyanurate (TMICN), dopamine hydrochloride, phenethylamine, acryloyl chloride, and 2,2-dimethoxy-2-phenylacetone (DMPA) were purchased from Sigma-Aldrich and used without further purification. Triethylamine (TEA) was purchased from Sigma-Aldrich and purified by drying with calcium hydride, followed by vacuum distillation. Anhydrous grade tetrahydrofuran, dimethylformamide, methanol, and ethyl acetate were purchased and used as received. DAC and PAC were synthesized from dopamine hydrochloride and phenethylamine, respectively, by reacting with acryloyl chloride [27, 28]. The detailed procedure is available in the supporting information with the corresponding NMR spectra (figures S1 and S2). All monomers used in this work are shown in figure 1.

2.2. Synthesis of thiol-ene/acrylamide SMP films

Using trifunctional monomers TMICN and TATATO and monofunctional acrylamides DAC and PAC, thiol-ene/acrylamide SMPs were synthesized by photopolymerization. Thiol, alkene, each acrylamide monomer, and 1 wt% DMPA of total monomer weight were dissolved in a glass vial using a spin mixer. DAC and PAC were counted as alkene components, and their monomer ratios varied from 0 to 40 mol% at 10 mol% increments. The stoichiometric balance between thiol and ene was maintained by correcting the number of functional groups in each monomer, as described in table 1. The monomer solution was encased between two glass slides spaced by 30 μm thick plastic shims of varying thickness to accommodate for different tests, then polymerized in a 254 nm UV curing chamber for 2 h. The cured polymer was heated in a vacuum oven at 120 $^{\circ}\text{C}$ and 150 mmHg for 24 h to complete the reaction.

2.3. Dynamic mechanical analysis (DMA)

DMA measurements were performed under tensile mode using an RSA-G2 (TA Instruments) with a maximum strain of 0.275%, deformation frequency of 1 Hz, and ramp rate of 2 $^{\circ}\text{C min}^{-1}$ in air (dry conditions) or in phosphate-buffered saline (PBS) (soaked/wet conditions). The test samples were cut into a rectangle 30 μm in thickness, 15 mm in length,

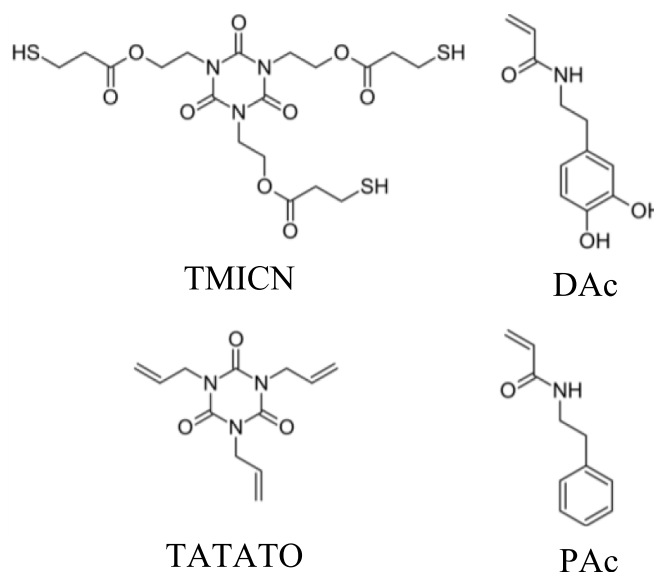


Figure 1. Chemical structures of monomers.

and 3 mm in width using a CO_2 laser. Dry DMA experiments were performed from 5 $^{\circ}\text{C}$ to 100 $^{\circ}\text{C}$. Soaked experiments consisted of two steps with the immersion system of the DMA instrument filled with PBS [29]. The first step was the complete immersion of the polymer. The temperature was raised from room temperature 22 $^{\circ}\text{C}$ to 37 $^{\circ}\text{C}$, then maintained for 60 min. In this process, the softening kinetics were evaluated, and the completion of softening process was confirmed through a steady modulus. The second step included cooling to 15 $^{\circ}\text{C}$, followed by heating from 15 $^{\circ}\text{C}$ to 80 $^{\circ}\text{C}$ to observe the thermomechanical properties under wet conditions after the polymer is plasticized. All measurements were performed for three independent specimens to obtain mean value and standard deviation; however, only representative measurements are shown in the graphics. The glass transition temperature (T_g) was evaluated at the $\tan \delta$ peak. Values are displayed as mean \pm standard deviation.

2.4. Tensile tests

Stress-strain curves were obtained using a universal testing machine (Lloyd LR5K Plus), which has a temperature-controlled chamber. Polymer samples were made according to the previously described procedure as 1.25 mm thick sheets. The sheets were cut into ASTM D638 Type V dogbones via a CO_2 laser. Each sample was tested at $T_g + 20$ $^{\circ}\text{C}$, and all samples were heated in the chamber at the corresponding temperature for 10 min prior to the measurements. The results were recorded using a 50 N load cell at a strain rate of 0.87%/s (5 mm min^{-1} extension speed). Each polymer was measured five times, and values including fracture strain (ϵ_f) and Young's modulus (E) at $T_g + 20$ $^{\circ}\text{C}$ were averaged.

2.5. Shape memory tests

A. Dry conditions: To test shape memory behavior, samples were cut by a carbon dioxide (CO_2) laser from thin polymer

Table 1. Thermomechanical and mechanical properties of the SMPs modified by DAc and PAc.

	Monomer compositions (mol% of functional groups)				T_g (°C)	E at $T_g + 20$ °C (MPa)	ε_f $T_g + 20$ °C (%)	E_r' (MPa)	ρ_x [$\times 10^{-3}$ mol cm $^{-3}$]
	TMICN	TATATO	DAc	PAc					
1	100	100			59.4 ± 0.6	6.7 ± 0.4	75.0 ± 3.6	19.1 ± 0.3	2.06
2		90	10		53.9 ± 0.4	4.1 ± 0.4	83.1 ± 3.2	12.3 ± 0.2	1.34
3		80	20		52.6 ± 0.6	3.0 ± 0.1	100.3 ± 2.1	8.0 ± 0.2	0.877
4		70	30		51.2 ± 0.4	2.0 ± 0.1	108.8 ± 2.7	4.85 ± 0.1	0.533
5		60	40		44.0 ± 0.4, 26.9 ± 0.2	0.8 ± 0.1	147.9 ± 12.4	2.68 ± 0.1	0.300
6		90		10	55.5 ± 0.7	5.9 ± 0.4	86.1 ± 4.5	13.1 ± 0.2	1.42
7		80		20	53.8 ± 0.4	4.2 ± 0.9	90.6 ± 6.3	11.1 ± 0.3	1.21
8		70		30	52.7 ± 0.5	3.5 ± 0.1	97.4 ± 8.8	7.53 ± 0.2	0.826
9		60		40	47.7 ± 0.4, 35.6 ± 0.3	2.2 ± 0.5	128 ± 12.1	4.18 ± 0.2	0.464

Values are expressed in mean ± standard deviation for $n = 3$ measurements each.

sheets into square strips (125 $\mu\text{m} \times 3 \text{ mm} \times 20 \text{ mm}$ in thickness, width, and length, respectively). A series of cyclic thermomechanical tests were performed to evaluate shape recovery behavior using an RSA-G2 (TA Instruments). The temperature ramping rate was 2 °C min $^{-1}$ in each process, and the test was conducted using the following steps. (a) The sample was heated to $T_g + 20$ °C and (b) stretched to strain (ε) = 50% at a constant strain rate of 0.1%/s; the maximum strain (ε_m) in loading was recorded after stretching. (c) The sample was cooled to 25 °C under constant strain, then unloaded, and the strain after unloading at a low temperature (ε_u) was obtained. (d) The sample was reheated to $T_g + 20$ °C under no load, and the temperature was maintained for 30 min; the strain after shape recovery from heating to T_g (ε_r) was obtained. The shape fixity (R_f) and recovery ratios (R_r) were defined by the following equations [30]:

$$R_f = \varepsilon_u / \varepsilon_m \times 100 (\%), \quad (1)$$

$$R_r = (\varepsilon_u - \varepsilon_r) / \varepsilon_u \times 100 (\%). \quad (2)$$

B. Wet conditions: A flat rectangular specimen (the permanent shape, 30 $\mu\text{m} \times 3 \text{ mm} \times 20 \text{ mm}$ in thickness, width, and length, respectively) was bent to 180° at $T_g + 20$ °C using glass plates with a radius of curvature of 470 μm (maximum strain $\approx 3\%$) and then cooled to room temperature (22 °C) under the external force to maintain the deformation. The deformed specimen was immersed in PBS at 37 °C, and the evolution of the recovered angle (θ_r) with time was recorded. R_r was defined by the following equation [30, 31]:

$$R_r = (180^\circ - \theta_r) / 180^\circ. \quad (3)$$

The detailed setup of the test is shown in the supporting information (figure S3).

3. Results and discussion

3.1. Thermomechanical and mechanical properties

The monomer molar ratios of DAc and PAc varied from 0 to 40 mol% at 10 mol% increments while maintaining a stoichiometric balance between thiol and ene. The thermomechanical properties of the synthesized polymers were evaluated using DMA (figure 2).

All polymers exhibited typical curves for thermoplastic polymers. The polymers were in a glassy state at room temperature (22 °C), softened at around T_g , and finally formed a rubbery plateau region at higher temperatures. The crosslinking density (ρ_x) of the polymer was calculated from the rubbery plateau storage modulus (E_r'), which is E' at $T_g + 40$ °C from DMA data in accordance with the theory of rubbery elasticity using equation (4):

$$\rho_x = E_r' / \{2(1 + \nu)RT\} \quad (4)$$

where R is the gas constant, T is the absolute temperature at which E_r' was measured, and ν is the Poisson's ratio, which is assumed to be 0.5 (incompressible materials) [27, 32]. T_g , E_r' , and ρ_x are summarized with monomer compositions in table 1.

T_g (given by the peak of $\tan \delta$) and E' in the rubbery state decreased as the DAc molar ratio increased. The decrease in T_g and E' can be attributed to the lower ρ_x of the polymer network due to the introduction of monofunctional DAc into the trifunctional TMICN and TATATO system [33]. Acrylamides have an alkene component: and thus can be incorporated into thiol-ene reaction systems [28, 34]. However, the free radical reaction system comprising thiol, alkene, and acrylamide may result in a heterogeneous polymer network because the ternary thiol-ene reaction and homopolymerization of the acrylamide proceed simultaneously [35]. The $\tan \delta$ curves became broader as the DAc ratio increased, implying that DAc provided a more heterogeneous polymer network. The two peaks in the $\tan \delta$ curve of the 40 mol% DAc-modified polymers are attributed

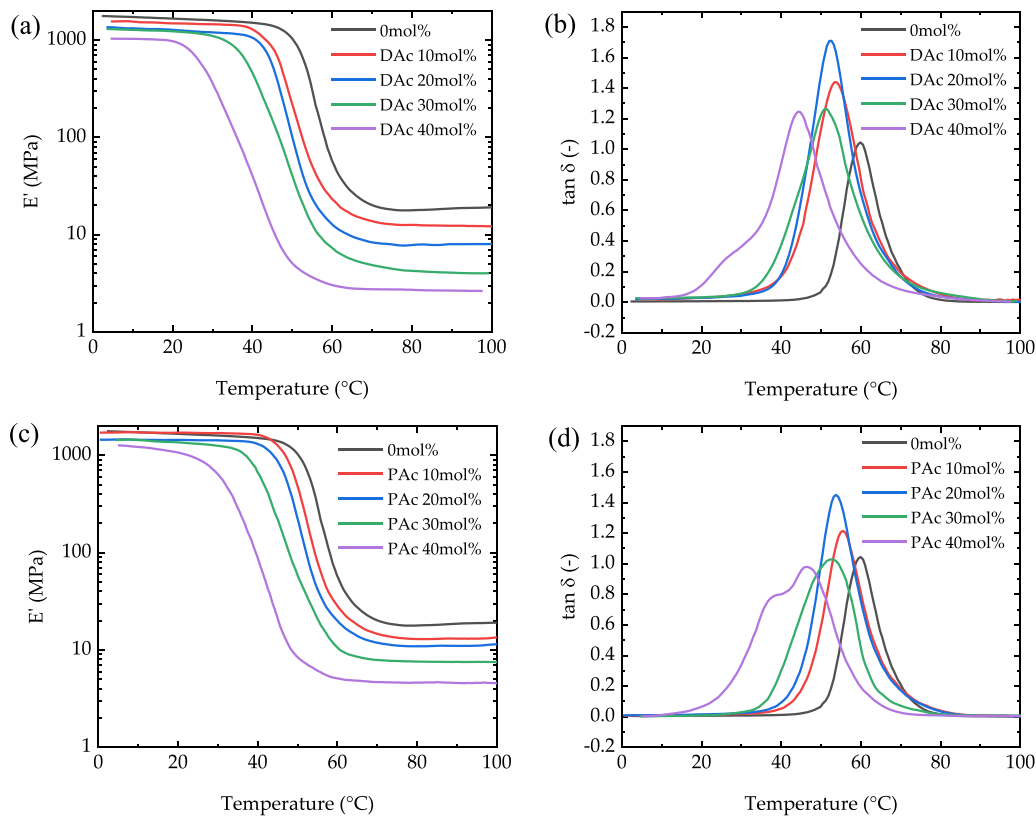


Figure 2. Thermomechanical properties of modified SMPs under dry conditions (a) E' , (b) $\tan \delta$ for DAC, and (c) E' , (d) $\tan \delta$ for PAC.

to phase separation in the polymer network. For the 40 mol% DAC-modified polymer, room temperature (22 °C) was close to the onset temperature, and E' at 22 °C dropped to approximately 880 MPa. Therefore, 40 mol% is the maximum amount of DAC that can be added while maintaining good handling properties for implantation. T_g and E' in the rubbery state decreased with increasing PAC molar ratio, similar to the DAC-modified polymers. Although the polymers modified with DAC and PAC had almost the same thermomechanical properties for the same molar ratios, T_g and E' of the DAC-modified polymers were slightly higher than those of the PAC-modified polymers. It is well known that unprotected catechol groups act as radical scavengers to interfere with radical reactions [36]. Patton's group reported that the conversion of monomers decreased as the DAC molar ratio increased for a ternary thiolene/acrylamide system, which consisted of pentaerythritol tetra(3-mercaptopropionate) as a thiol (PETMP), pentaerythritol triallyl ether (APE) as an alkene, and DAC, in their real-time Fourier-transform infrared spectroscopy study of ultraviolet (UV) photopolymerization [27]. In contrast, PAC-modified polymers retained higher conversions. The difference between the modification effects of DAC and PAC in this study can be ascribed to the same interference effect of the catechol residue because the result is consistent with a previous study by Patton *et al.* Interestingly, however, we could observe a decrease in T_g with increasing DAC content, while they found an increase. For the addition of PAC, the same trend (decrease in T_g) was observed for both studies. This can be explained

by the more rigid polymer structure of the TMICN-TATATO network than that of APE-PETMP. TMICN and TATATO have more rigid isocyanurate residue instead of pentaerythritol residue for APE and PETMP. Physical crosslinks through hydrogen bonds between hydroxyl groups and ester/amide carbonyls within the polymer network can be formed less effectively because of the lower flexibility of the TMICN-TATATO network structure. By introducing the monofunctional monomers DAC or PAC, the thermomechanical properties of the resulting polymers are dominated by the decrease in crosslinking density and the increase in chain mobility and flexibility. Therefore, the addition of both monomers caused a decrease in T_g as opposed to the previous work by Dr Patton's group. Due to the same reasons, namely the decreased rotational freedom of TATATO and TMICN compared to APE and PETMP, we could achieve much higher T_g 's overall.

Next, the mechanical properties at $T_g + 20$ °C were evaluated using tensile tests to determine the measurement conditions for the shape recovery behavior explained in the next section (table 1). The respective stress-strain curves can be found in Supplemental figures S4 and S5. As the DAC and PAC molar ratios increased, the Young's modulus (E) decreased, but the fracture strain (ε_f) increased. Furthermore, compared to the PAC-modified polymers, E was lower, but ε_f was higher for the DAC-modified polymers. These results are in good agreement with the discussion of the DMA data regarding crosslinking density and conversion.

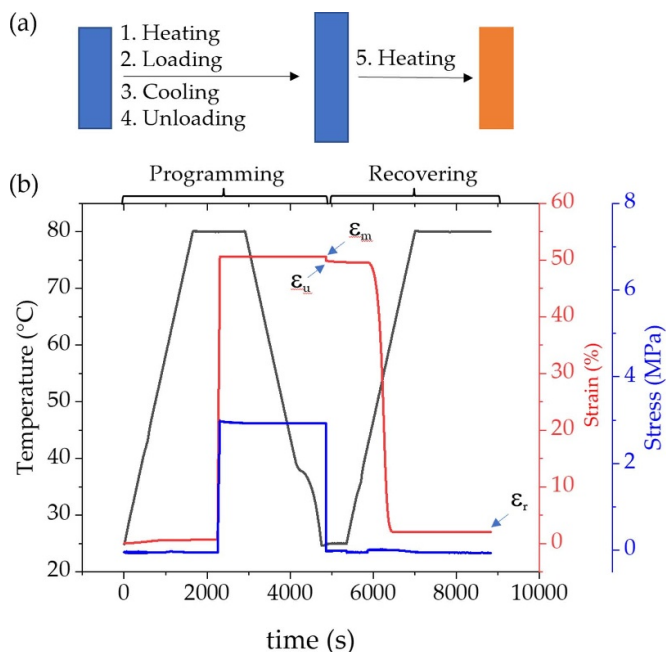


Figure 3. Thermo-responsive shape memory effect is demonstrated through (a) a schematic diagram and (b) thermomechanical analysis diagram.

3.2. Shape recovery properties under dry conditions

The molecular structure of an SMP is composed of crosslinking points, also called net points, and switching segments interconnected by crosslinking points [30, 37]. The original shape of the SMP is fixed by crosslinking points formed during polymerization and is also called the permanent shape. Switching segments soften above the transition temperature (T_t) and help the polymer deform easily. After deformation and cooling to below T_t , the motion of the polymer chains is ‘frozen’ to fix the temporary shape of the SMP. Although the temporary shape is a metastable state and entropically unfavored, the shape recovery to the permanent shape is inhibited because the polymer chains’ motion is restricted below T_t . When the SMP is reheated to T_t , the polymer chains can move, and the stored energy is released; then, the shape recovers to the permanent shape. This study assessed the shape memory behavior under dry conditions under strain-controlled cyclic thermomechanical measurements. The strain for fixing the temporary shape was set to 50% because the smallest ϵ_f of all the synthesized polymers was 75% for the unmodified SMP, and T_t was defined as $T_g + 20^\circ\text{C}$ for each polymer. The polymers at each step during the test and the quantitative thermomechanical analysis diagram for the unmodified polymer are shown as representative data in figure 3.

Each polymer was heated from room temperature (22°C) to $T_g + 20^\circ\text{C}$ and stretched to $\epsilon = 50\%$, then cooled to 22°C under constant load to fix its shape as the temporary shape. Afterward, the polymer was reheated to $T_g + 20^\circ\text{C}$ to activate shape recovery (figures S6–S9). The shape fixity ratio (R_f) and recovery ratio (R_r) for the SMPs were calculated from the changes in the strain at each step [30, 38] (figure 4).

Adding DAc and PAc had very similar effects on the shape memory properties. Both R_f and R_r remained unchanged up to 30 mol% for both DAc and PAc (98% and 95%, respectively). At 40 mol%, R_f remained relatively constant, but R_r decreased to approximately 90%. All SMPs returned to the glassy state after cooling to room temperature (22°C) to fix the temporary shape. Therefore, their frozen polymer chains restrict spring back, which can be caused by internal stress, thus maintaining a high R_f [17, 39]. The SMP in the temporary state has a more ordered arrangement of polymer chains and is entropically unfavored. When heating, the SMP returns to the original shape, driven by regaining the entropy [40, 41]. The reduction of entropy, which is the driving force for shape recovery, becomes smaller as the crosslinking density decreases [42]. Consequently, the lower driving force reduced R_r at 40 mol%. Overall, the polymers modified by DAc and PAc showed very similar Shape recovery performances, as expected from the thermomechanical and mechanical analysis data.

3.3. Thermomechanical properties under wet conditions

The thermomechanical properties of the SMPs under wet conditions were evaluated using soaked DMA, which measured a sample while immersed in PBS (figure 5).

Under wet conditions, T_g decreased for all polymers compared to that under dry conditions. It is well known that water molecules that penetrate polymers often act as a plasticizer, increasing the mobility of polymer chains and the free volume of polymers to reduce T_g and E' [43]. T_g of unmodified polymer decreased from 59.9°C under dry conditions to 44.0°C under wet conditions. Both T_g values are higher than the body temperature (37°C); therefore, the polymer was in the transition state from the glassy to the rubbery state and softened only to 215 MPa under physiological conditions (i.e. immersed in PBS at 37°C). However, the T_g values of the polymers modified with 10, 20, 30, and 40 mol% DAc decreased considerably to 32.2 , 27.9 , 24.0 , and 22.0°C and softened to 11, 6.1, 3.7, and 2.1 MPa, respectively. The modification by PAc also decreased T_g and E' , but the softening effect was weaker than that of DAc. Specifically, for the 40 mol% PAc-modified polymers, T_g and E' were 22°C and 3.8 MPa under physiological conditions, respectively. Even though the PAc-modified polymers exhibited nearly identical thermomechanical properties to those of the DAc-modified polymers under dry conditions, as previously described, there was a significant difference under wet conditions. This is attributed to the difference in their hydrophilicity. It is suggested that the DAc-modified polymers were more affected by plasticization from water because they were more hydrophilic and had a higher affinity for water than the PAc-modified polymers.

To investigate the hydrophilicity of the polymers, the surface free energy and swelling ratio under physiological conditions were evaluated. The surface free energy was calculated using the Owens, Wendt, Rable, and Kaelbel method [44], which is a representative method for analyzing the energy of the surface of a solid. This method assumes that the surface energy consists of dispersive (γ_d) and polar parts (γ_p),

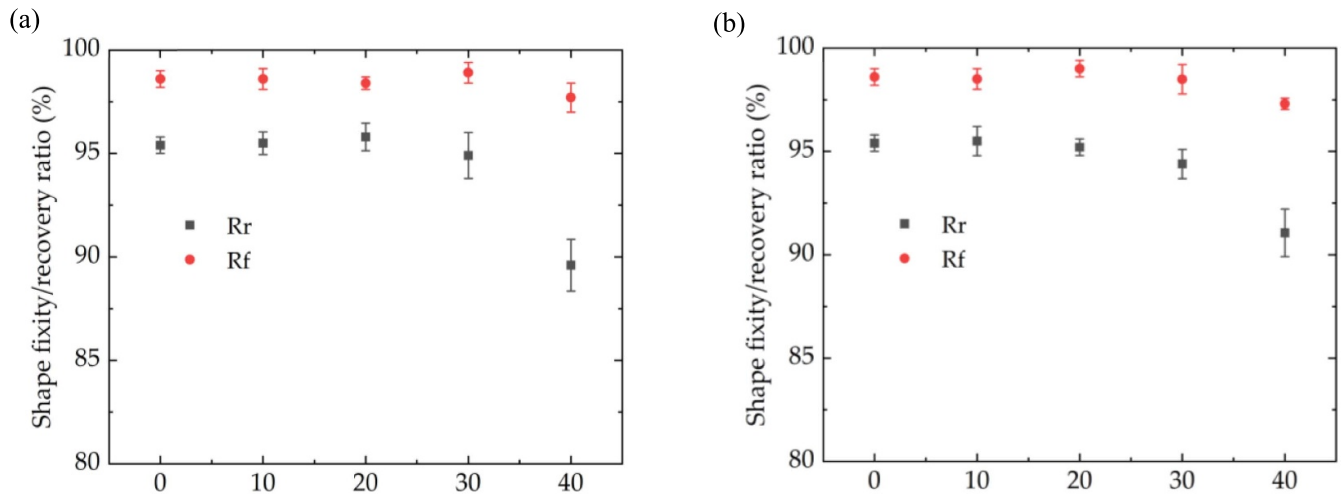


Figure 4. Shape fixity (R_f) and shape recovery (R_r) ratio of SMPs under dry condition of (a) DAC-modified and (b) PAc-modified polymers. Mean values and standard deviations are shown for $n = 3$ measurements each.

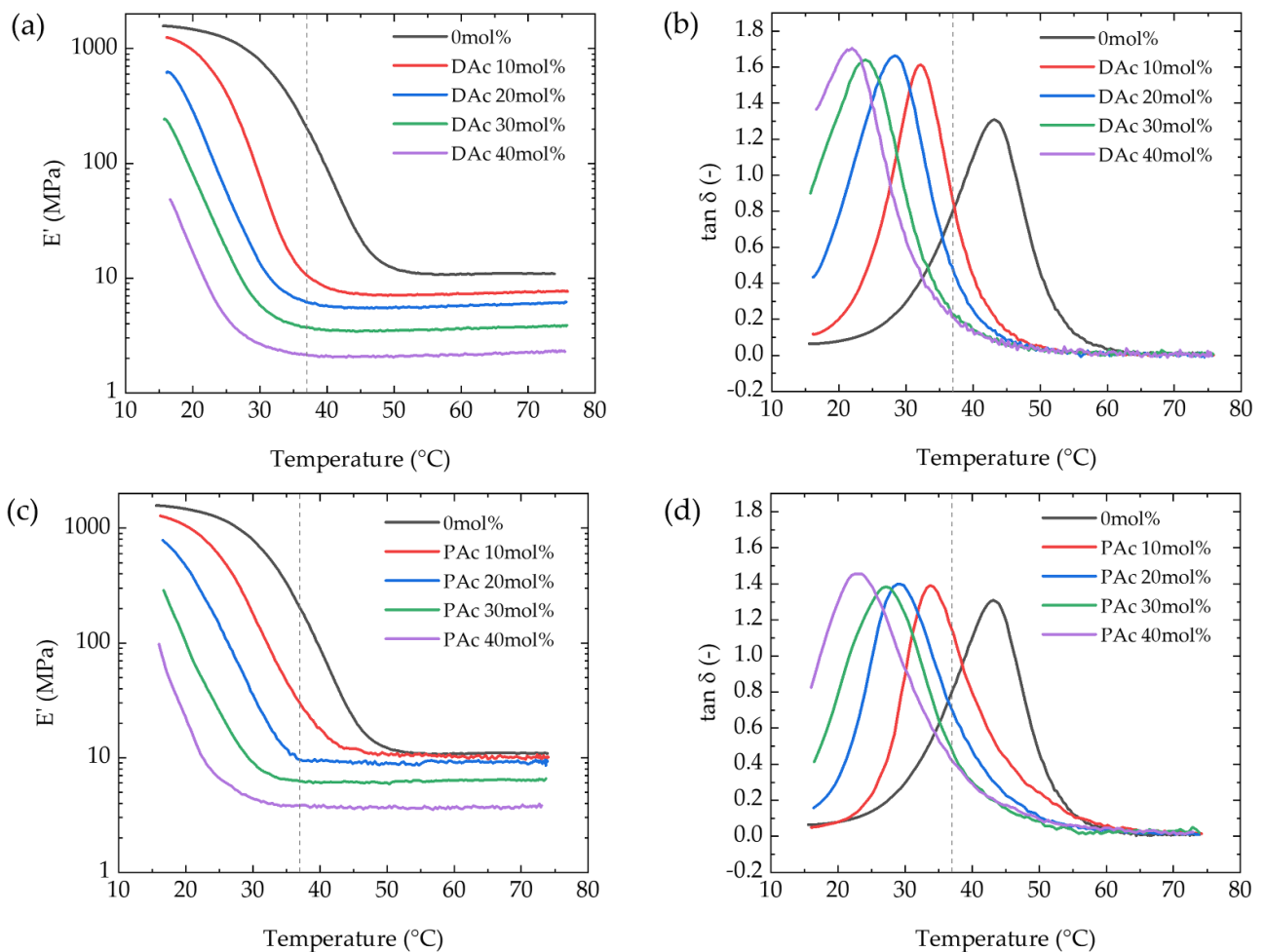


Figure 5. Thermomechanical properties of modified SMPs under wet conditions (a) E' ; (b) $\tan \delta$ for DAC; (c) E' ; (d) $\tan \delta$ for PAc.

which can be calculated from the measured contact angles for two probe liquids with different γ_d and γ_p values. In this work, water and diiodomethane were used, which are a widely used combination for this method (table S1) [38]. For the

DAC-modified polymers, both γ_d and γ_p increased as the DAC molar ratio increased, while modification by PAc increased γ_d but decreased γ_p (figure S10). DAC modification increased γ_d and γ_p mainly owing to the benzene ring and two hydroxyl

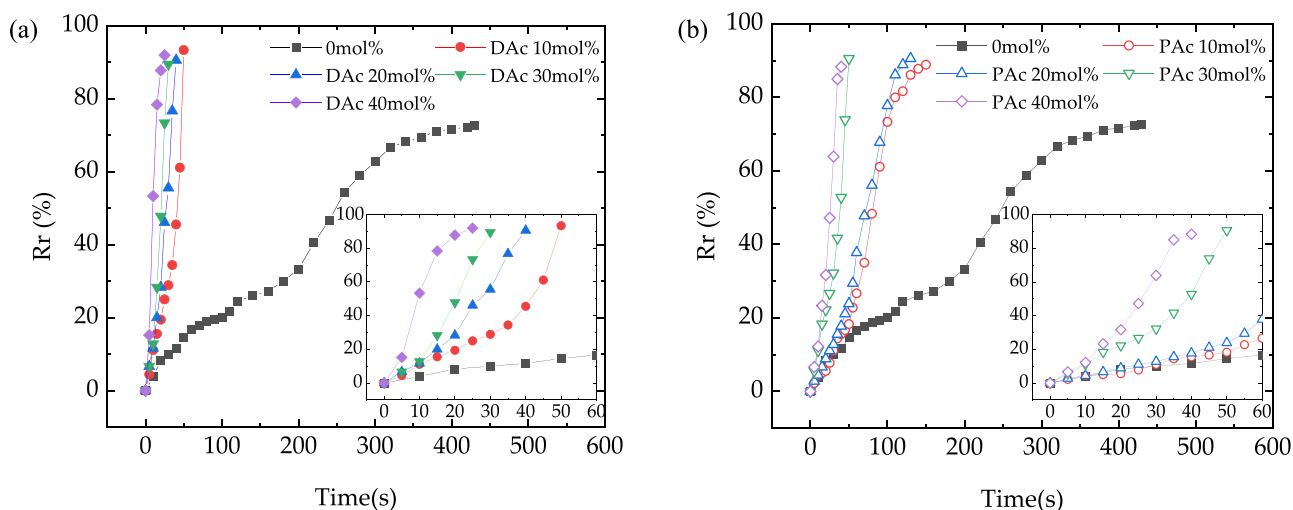


Figure 6. Shape recovering behavior under physiological conditions for (a) DAc-modified, and (b) PAc-modified SMPs. Inset shows magnified initial sections of each curve.

groups in the catechol group, respectively. Unlike DAc, PAc does not have two hydroxyl groups; therefore, γ_p decreased due to the benzene ring's low polarity. These results indicate that DAc made the SMPs more hydrophilic, whereas PAc made them more hydrophobic. Next, the swelling ratios of the SMPs under physiological conditions were measured by immersing the SMPs in PBS at 37 °C. Although PAc increased the hydrophobicity of the polymer, the swelling ratio increased for the polymers modified with at least 30 mol% PAc (figures S11, S12) because the lower crosslinking density increased the free volume of the polymers [43]. The addition of DAc increased the swelling ratio even more than the addition of PAc. For instance, the swelling ratio of the 10 mol% DAc-modified SMP was $2.2 \pm 0.23\%$, which was as high as that of the 40 mol% PAc-modified SMP. This result is attributed to the enhanced hydrophilicity and reduced crosslinking density due to the addition of DAc.

3.4. Shape recovery properties under wet conditions

The shape recovery properties of the synthesized SMPs under physiological conditions were evaluated in PBS at 37 °C. A flat rectangular SMP sheet ($30 \mu\text{m} \times 3 \text{ mm} \times 20 \text{ mm}$ in thickness, width, and length, respectively) (the permanent shape) was heated and bent to a U-shape (the temporary shape). Then, the SMP was fixed in the temporary shape by cooling under load. The recovery behavior of the SMP from U-shape to flat in the PBS bath was recorded (figure S13), and R_r was calculated from the change in angle at each time point (figure 6) [31].

When the SMP was exposed to physiological conditions, a temperature increase from room temperature (22 °C) to 37 °C and water absorption occurred simultaneously. Softening from both water absorption and the temperature increase triggered shape recovery under physiological conditions [45]. The shape recovery process for the unmodified polymer was very slow. R_r reached only approximately 70% in 300 s, and there was no significant change after that. As mentioned in the previous

section, R_r was approximately 95% under dry conditions when the SMP was activated by heating to $T_g + 20$ °C. These results show that exposure to physiological conditions did not have a sufficient driving force for shape recovery of the SMP. This is reasonable because the T_g of the unmodified SMP under wet conditions was 44 °C, which is higher than 37 °C. The addition of DAc and PAc improved the shape recovery properties. This effect is ascribed to decreases in the crosslinking density and T_g after modification, which would accelerate shape recovery because of the lower onset temperature for softening. The SMP modified with only 10 mol% DAc attained $R_r = 90\%$ in only 40 s, and the shape recovery behavior improved further with increasing DAc molar ratio. The 40 mol% DAc-modified polymer reached $R_r = 90\%$ in only 20 s. PAc also improved the shape recovery effect. However, the effect of DAc was considerably higher than that of PAc, and the difference was pronounced when the molar ratios were small. This result is attributed to the enhanced hydrophilicity from DAc modification.

3.5. Softening kinetics

The experimental results of the thermomechanical properties from soaked DMA and the swelling ratio that we have discussed thus far are the properties of the SMPs after water absorption reaches the equilibrium state. However, it is highly probable that the shape recovery under physiological conditions would proceed under non-equilibrium conditions because the recovery would be activated while T_g and E' continued to drop owing to the temperature increase and water absorption until the SMP fully softened. Thus, evaluating the softening kinetics of the SMPs under physiological conditions has great significance for a more detailed discussion about the non-equilibrium softening process. Therefore, we observed the softening profiles by evaluating the change in E' with time after soaking the SMPs in PBS using a soaked DMA instrument, which is a procedure established in previous work [29] conducted by Voit's group (figure 7).

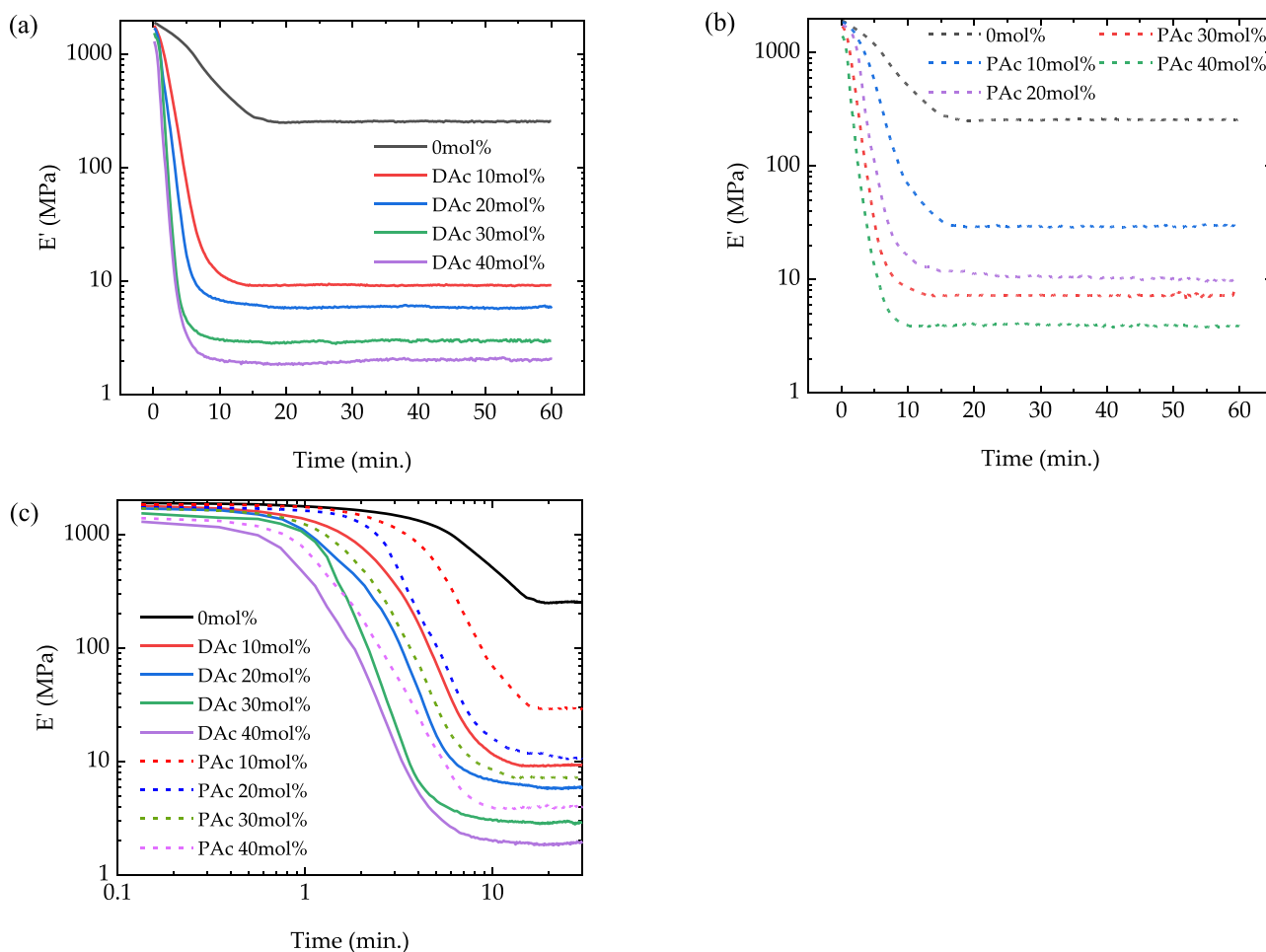


Figure 7. Softening profiles of (a) DAC-modified, (b) PAC-modified SMPs, and (c) logarithmic scale of time to show onset temperature with varying monomer composition.

The unmodified polymer started to soften at $t = 3$ min and completely softened at $t = 19$ min to reach the equilibrium state. The onset time for softening decreased as the DAC molar ratio increased, and E' also decreased after complete softening. The 40 mol% DAC-modified polymer, which had the highest DAC ratio, began to soften at $t = 0.5$ min and fully softened in only 8 min. PAC induced a similar effect on softening, but the strength of the effect was lower than that of DAC. The 40 mol% PAC-modified polymer completely softened in approximately 10 min. These experimental results were strongly correlated with the shape recovery behavior under physiological conditions. Therefore, we can conclude that the improved hydrophilicity and reduced T_g under wet conditions enabled faster softening, which resulted in substantially faster shape recovery.

3.6. Biocompatibility tests

The biocompatibility of the polymers is also crucial because they were designed for implantable devices. It was tested based on the MTT (3-(4,5-dimethylthiazol-2-yl)-2,5-diphenyltetrazolium bromide) assay for the unmodified, 40 mol% DAC-modified, and 40 mol% PAC-modified

polymers. In the MTT assay, succinate dehydrogenase in the mitochondria of live cells converts yellow MTT to purple MTT-formazan. The dehydrogenase is involved with the respiratory chain; therefore, the activity of the enzyme, which is estimated from the optical density at 570 nm (OD570), can be an indicator of cell viability. The cell viabilities estimated from the MTT assay for each polymer were $88.4 \pm 7.4\%$, $91.5 \pm 10.8\%$, and $91.2 \pm 4.0\%$ for the unmodified, 40 mol% DAC-modified, and 40 mol% PAC-modified polymers, respectively (figure S14). Based on ISO 10993-5 [46], when the viability is lower than 70%, the material is considered cytotoxic. Therefore, it was confirmed that the 40 mol% DAC- and 40 mol% PAC-modified polymers and unmodified polymers were biocompatible. If modification by DAC and PAC induced cytotoxicity, adding 40 mol% should provide the worst result. Hence, all the polymers in this work were biocompatible.

4. Conclusion

In this study, we designed new thiol-ene/acrylamide SMPs using DAC as a hydrophilic monomer to control the thermomechanical properties and hydrophilicity of current thiol-ene SMPs. Soaked DMA and observation of shape recovery

under physiological conditions revealed that DAc significantly improved both the softening effect and shape recovery properties. The softening kinetics study of the SMPs under physiological conditions clearly showed that the onset and completion times for softening decreased as the DAc molar ratio increased. Furthermore, MTT assays confirmed that these modified SMPs were biocompatible. The improved softening and shape recovery effect can be utilized for self-implantation and fixation of neural interface devices for minimally invasive implantation. 40 mol% DAc-modified polymer exhibited a drastic decrease in E' from 880 MPa to 2.1 MPa after exposure to physiological conditions and rapidly triggered shape recovery, which is a suitable candidate for future applications. Here, we propose a new design guideline that makes thiol-ene SMPs better candidates for flexible substrates for neural interfaces.

Data availability statement

The data that support the findings of this study are available upon reasonable request from the authors.

ORCID iDs

Walter Voit  <https://orcid.org/0000-0003-0135-0531>

Melanie Ecker  <https://orcid.org/0000-0002-0603-6683>

References

- [1] Zhang M, Tang Z, Liu X and Van der Spiegel J 2020 *Nat. Electron.* **3** 191–200
- [2] Hochberg L R, Serruya M D, Friehs G M, Mukand J A, Saleh M, Caplan A H, Branner A, Chen D, Penn R D and Donoghue J P 2006 *Nature* **442** 164–71
- [3] Alahi M E E, Liu Y, Xu Z, Wang H, Wu T and Mukhopadhyay S C 2021 *Mater. Today Commun.* **29** 102853
- [4] Hong Y J, Jeong H, Cho K W, Lu N and Kim D-H 2019 *Adv. Funct. Mater.* **29** 1808247
- [5] Bettinger C J 2018 *Bioelectron. Med.* **4** 6
- [6] Hoogerwerf A C and Wise K D 1994 *IEEE Trans. Biomed. Eng.* **41** 1136–46
- [7] Nordhausen C T, Maynard E M and Normann R A 1996 *Brain Res.* **726** 129–40
- [8] Renz A F, Reichmuth A M, Stauffer F, Thompson-Steckel G and Vörös J 2018 *J. Neural Eng.* **15** 061001
- [9] Hassler C, Boretius T and Stieglitz T 2011 *J. Polym. Sci. B* **49** 18–33
- [10] Noh H, Moon K, Cannon A, Hesketh P J and Wong C P 2004 *Proc. 54th Electronic Components and Technology Conf. (IEEE Cat. No. 04CH37546)* vol 1 pp 924–30
- [11] Seymour J P, Langhals N B, Anderson D J and Kipke D R 2011 *Biomed. Microdevices* **13** 441–51
- [12] Nemani K V, Moodie K L, Brennick J B, Su A and Gimbi B 2013 *Mater. Sci. Eng. C* **33** 4453–9
- [13] McClain M A, Clements I P, Shafer R H, Bellamkonda R V, LaPlaca M C and Allen M G 2011 *Biomed. Microdevices* **13** 361–73
- [14] Ecker M, Joshi-Imre A, Modi R, Frewin C L, Garcia-Sandoval A, Maeng J, Gutierrez-Heredia G, Pancrazio J J and Voit W E 2019 *Multifunct. Mater.* **2** 012001
- [15] Garcia-Sandoval A et al 2018 *J. Neural Eng.* **15** 045002
- [16] Ware T et al 2012 *Macromol. Mater. Eng.* **297** 1193–202
- [17] Zhang Y et al 2019 *Sci. Adv.* **5** eaaw1066
- [18] González-González M A et al 2018 *Sci. Rep.* **8** 16390
- [19] Wu X L, Kang S F, Xu X J, Xiao F and Ge X L 2014 *J. Appl. Polym. Sci.* **131** 40559
- [20] Wei Y, Huang R, Dong P, Qi X-D and Fu Q 2018 *Chin. J. Polym. Sci.* **36** 1175–86
- [21] Tekay E 2020 *Polymer* **209** 122989
- [22] Yan N, Zheng Z, Liu Y, Jiang X, Wu J, Feng M, Xu L, Guan Q and Li H 2022 *Nano Res.* **15** 1383–92
- [23] Lee Y B, Shin Y M, Lee J-H, Jun I, Kang J K, Park J-C and Shin H 2012 *Biomaterials* **33** 8343–52
- [24] Kim S, Jang L K, Park H S and Lee J Y 2016 *Sci. Rep.* **6** 30475
- [25] Kang S M, You I, Cho W K, Shon H K, Lee T G, Choi I S, Karp J M and Lee H 2010 *Angew. Chem., Int. Ed.* **49** 9401–4
- [26] Pfau M R and Frunlan M A 2021 *J. Mater. Chem. B* **9** 4287–97
- [27] Sparks B J, Hoff E F T, Hayes L P and Patton D L 2012 *Chem. Mater.* **24** 3633–42
- [28] Nishida J, Kobayashi M and Takahara A 2013 *ACS Macro Lett.* **2** 112–5
- [29] Hosseini S M, Voit W E and Ecker M 2019 *J. Vis. Exp.* **145** e59209
- [30] Lendlein A and Kelch S 2002 *Angew. Chem., Int. Ed.* **41** 2034–57
- [31] Kong D and Xiao X 2016 *Sci. Rep.* **6** 33610
- [32] Flory P J 1979 *Polymer* **20** 1317–20
- [33] Safranski D L and Gall K 2008 *Polymer* **49** 4446–55
- [34] Lowe A B 2010 *Polym. Chem.* **1** 17–36
- [35] Senyurt A F, Wei H, Phillips B, Cole M, Nazarenko S, Hoyle C E, Piland S G and Gould T E 2006 *Macromolecules* **39** 6315–7
- [36] Zafar S, Ahmed R and Khan R 2016 *Free Radic. Res.* **50** 939–48
- [37] Meng H and Li G 2013 *Polymer* **54** 2199–221
- [38] Xie T 2011 *Polymer* **52** 4985–5000
- [39] Li F, Zhu W, Zhang X, Zhao C and Xu M 1999 *J. Appl. Polym. Sci.* **71** 1063–70
- [40] Anthamatten M, Roddecha S and Li J 2013 *Macromolecules* **46** 4230–4
- [41] Hornat C C and Urban M W 2020 *Prog. Polym. Sci.* **102** 101208
- [42] Cowie J M G and Arrighi V 2007 *Polymers: Chemistry and Physics of Modern Materials* 3rd edn (Florida: CRC Press)
- [43] Tomar R S, Gupta I, Singhal R and Nagpal A K 2007 *Des. Monomers Polym.* **10** 49–66
- [44] Owens D K and Wendt R 1969 *J. Appl. Polym. Sci.* **13** 1741–7
- [45] Du H and Zhang J 2010 *Soft Matter* **6** 3370–6
- [46] ISO 10993-5 2009 *Biological Evaluation of Medical Devices—Part 5: Tests for in vitro Cytotoxicity*